

# Small Molecule Oxidation Products Trigger Disease-Associated Protein Misfolding

JAN BIESCHKE, QINGHAI ZHANG,  
DARYL A. BOSCO, RICHARD A. LERNER,  
EVAN T. POWERS,  
PAUL WENTWORTH, JR., AND  
JEFFERY W. KELLY\*

*The Scripps Research Institute,  
10550 North Torrey Pines Road, La Jolla, California 92037*

Received March 6, 2006

## ABSTRACT

Oxidative stress and inflammation are risk factors for both the development of  $\alpha$ -synucleinopathies, such as Parkinson's disease and dementia with Lewy bodies, and Alzheimer's disease, the two most common neurodegenerative disorders. These diseases are associated with the neurotoxic deposition of misassembled  $\alpha$ -synuclein and amyloid- $\beta$  ( $A\beta$ ) peptides, respectively. Both occur sporadically, that is, without detectable disease-related mutations, in the vast majority of cases. Small molecule oxidation products, especially secosterols derived from cholesterol and 4-hydroxy-nonenal derived from lipid peroxidation, found in afflicted brains, accelerate the misassembly of both  $A\beta$  and  $\alpha$ -synuclein. This Account explores the mechanism of small molecule oxidation product-mediated protein misassembly and possible intervention strategies.

## Introduction

The risk of developing a protein misfolding disease increases with age.<sup>1</sup> The amyloidoses are a major category of misfolding diseases involving the misassembly and deposition of toxic protein aggregates in various morphologies, including amyloid fibrils.<sup>2,3</sup> Protein misfolding diseases are subcategorized as intracellular or extracellular (although this distinction may not be useful if proteotoxicity arises from membrane structure perturbation). The most prominent "extracellular" amyloid disease is Alzheimer's disease (AD), whereas the most common intracellular misfolding diseases are the  $\alpha$ -synucleinopathies,

Jan Bieschke received his Ph.D. from the Max-Planck-Institute for Biophysical Chemistry in Göttingen, Germany (2000). He joined the laboratories of Hans Kretschmar in Munich, Germany (2000–2003), and then Jeffery Kelly (2003–2006) for postdoctoral research focusing on single molecule fluorescence and the mechanisms of protein folding and misfolding. He is now a Research Group Leader at the Max Delbrück Center for Molecular Medicine in Berlin.

Qinghai Zhang received his Ph.D. from the Shanghai Institute of Organic Chemistry, Chinese Academy of Sciences (2001). His postdoctoral research in the Kelly laboratory focused on the role of oxidative metabolites in triggering protein misfolding diseases (2001–2004). He is now an Assistant Professor in the Department of Molecular Biology at The Scripps Research Institute (TSRI) investigating membrane chemistry and biophysics.

Daryl Bosco received her Ph.D. in bio-organic chemistry from Brandeis University (2003). Her postdoctoral research (2003–2005) in the Kelly laboratory focused on oxidative metabolite initiated  $\alpha$ -synuclein misfolding. Daryl now works at Serono.

diseases including Parkinson's disease (PD) and dementia with Lewy bodies (DLB).<sup>4</sup> The amyloidoses typically exhibit tissue selective deposition and pathology; for example, the transthyretin amyloidoses either affect the peripheral nerves (neuropathies), the heart (cardiomyopathies), or the brain, depending on the mutant undergoing amyloidogenesis.<sup>5–9</sup>

Amyloid is an intermolecular fold available to most peptides and proteins.<sup>10,11</sup> X-ray crystallography, solid-state NMR, and hydrogen–deuterium exchange have recently been used to characterize the cross- $\beta$  sheet structure of various amyloid fibrils at atomic resolution.<sup>12–14</sup> However, smaller aggregation intermediates are also implicated in the toxicity of amyloidogenic proteins.<sup>1,15,16</sup> Different aggregation conditions favor different aggregate morphologies<sup>17</sup> from small spherical assemblies<sup>18</sup> to protofibrils.<sup>19</sup>

## Nucleated Polymerization Mechanism

Our understanding of amyloid fibril formation, while incomplete, suggests that aggregation can either be thermodynamically favored from the outset<sup>7</sup> or be characterized by a pronounced lag phase.<sup>20–22</sup> The lag phase of a nucleation-dependent polymerization<sup>19,23</sup> (Figure 1A) typically corresponds to slow formation of an oligomeric nucleus (Figure 1B). The steps preceding nucleation are energetically unfavorable because entropy loss outweighs the enthalpic gains from burial of hydrophobic surface area and H-bonding. Multivalent interactions occurring postnucleation are thought to render further monomer addition energetically favorable. Aggregates will not form

\* Corresponding author. E-mail: jkelly@scripps.edu.

Richard A. Lerner, President of The Scripps Research Institute, is the Lita Annenberg Hazen Professor of Immunochimistry, holds the Cecil H. and Ida M. Green Chair in Chemistry, and is a member of The Skaggs Institute for Chemical Biology. His research investigates the conversion of antibodies into enzymes and combinatorial methods for the synthesis of antibodies for therapeutic and catalytic purposes. Furthermore, he is interested in antibody facilitated ozone and reactive oxygen synthesis that can react with molecules in the body, such as cholesterol, to produce toxic compounds that induce protein misfolding.

Evan Powers received his Ph.D. in Organic Chemistry from the Massachusetts Institute of Technology (1999). He joined the Kelly lab in 1999 and became an Assistant Professor at TSRI in 2000. His main interests are the energetics and mechanisms of protein folding and aggregation.

Paul Wentworth, Jr. received his Ph.D. from the University of Sheffield, U.K. (1994). His postdoctoral experience was obtained at The Scripps Research Institute (TSRI) (1994–1997). He is now a Professor of Chemistry at TSRI and a Professor of Medicinal Chemistry at the University of Oxford, U.K. His interests include chemistry and biology of reactive oxygen and nitrogen species, inflammatory diseases, and mechanisms of protein misfolding and disease.

Jeffery W. Kelly received his Ph.D. from the University of North Carolina at Chapel Hill (1986) and performed postdoctoral research at The Rockefeller University. In 1989, he became Assistant Professor at Texas A&M University where he was subsequently promoted to Professor of Chemistry. He joined the Department of Chemistry at TSRI in 1997 as the Lita Annenberg Hazen Professor of Chemistry. He became Dean of Graduate Studies and Vice President of Academic Affairs in 2000. His research focuses on understanding protein folding and misfolding in vitro and in vivo and the influence of aging and small molecules on these processes.

below a critical concentration,  $K_c$ .<sup>20,21</sup> At peptide concentrations above  $K_c$ , aggregates grow until the monomer concentration decreases to  $K_c$  (see Figure 5C). The lag phase is eliminated when preformed fibrils or seeds are introduced into the reaction, obviating nucleation (Figure 1C). Energetically costly unimolecular conformational changes can also be required for monomeric nucleus formation.<sup>22</sup>

## Inflammatory Processes Are Implicated in Protein Misfolding Diseases

Familial protein misfolding diseases have provided important insights into pathogenesis. These diseases are typically caused by destabilizing mutations in amyloid prone proteins or in enzymes that process or degrade amyloidogenic peptides, such as  $\gamma$ -secretase or ubiquitin ligases.<sup>24</sup> While familial forms of AD and PD have been informative, the vast majority of AD and PD cases are sporadic, wherein the sequences of the misfolded proteins and interacting proteins are identical to those in persons without disease. Thus, epigenetic, environmental, or aging-associated factors<sup>1</sup> have to be considered. Extending Anfinsen's teachings suggests that either the environment immersing the chain could be different or an unusual post-translational modification could occur in patients with sporadic misfolding diseases.

Amide side chain deamidation is known to enhance amyloidogenicity,<sup>25</sup> however, little is known about the role of established bimolecular protein modifications mediated by aldehydic oxidative metabolites and similar molecules.<sup>26</sup> We hypothesize that aberrant post-translational protein modifications may trigger the onset of sporadic misfolding diseases by making amyloidogenesis more efficient, perhaps by changing the mechanism. Determining the factors exacerbating sporadic amyloidogenesis is key to slowing or preventing these diseases.

Epidemiological evidence suggests that inflammatory processes,<sup>27</sup> for example, those caused by traumatic brain injury<sup>28</sup> or mutations in pro-inflammatory cytokines,<sup>29,30</sup> promote AD. Levels of inflammation-related lipid peroxidation products are higher in AD.<sup>31,32</sup> The clinical use of nonsteroidal anti-inflammatory drugs (NSAIDs) appears to protect against the onset of AD.<sup>33</sup> Inflammation is also linked to PD<sup>34,35</sup> and possibly to DLB.<sup>36</sup> Anti-inflammatory drugs appear to exert a protective effect in mice treated with MPTP (1-methyl-4-phenyl-1,2,3,6-tetrahydropyridine), a drug that typically induces Parkinson's-like symptoms.<sup>34</sup> There is clear evidence for oxidative stress and lipid peroxidation in the blood of PD patients.<sup>37</sup>

## Lipid Peroxidation and the Generation of Reactive Aldehydes *in Vivo*

Lipid peroxidation in a biological setting results in the formation of aldehydic products.<sup>38,39</sup> Peroxidation proceeds via lipid alkoxyl radicals and is accelerated by transition metal ions such as  $Fe^{2+}$ ,  $Cu^+$ , and  $Co^{2+}$  (Figure 1D).<sup>38,40,41</sup> Some of these aldehydes produce pathologic effects *in vivo*. For example, 4-hydroxynonenal (4-HNE),

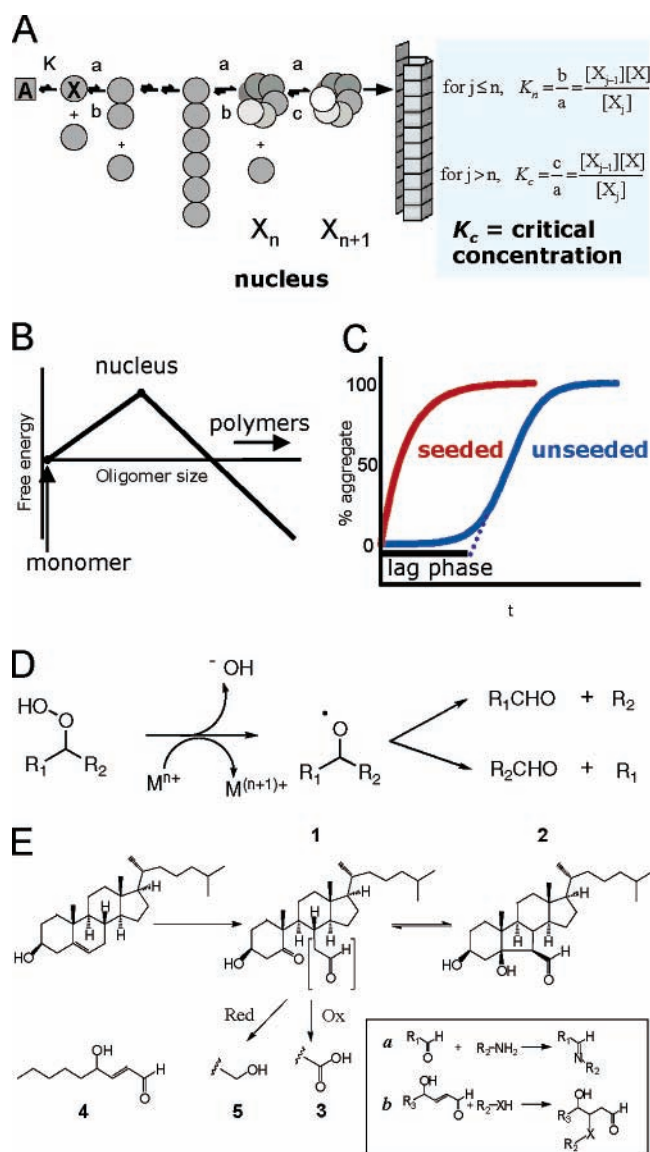


**FIGURE 1.** Nucleation dependent polymerization. (A) Elementary monomer addition reactions in fibrillogenesis. (B) Free energy diagram for oligomer formation, when the peptide concentration is higher than the critical concentration  $K_c$ . The free energy is a maximum for the nucleus. (C) Aggregation kinetics observed in nucleated polymerization. (D)  $\beta$ -Cleavage route of lipid hydroperoxides to aldehyde products. (E) Cholesterol is oxidized to form aldehyde (**1**), which rapidly equilibrates to the aldol (**2**) via Schiff base formation. Further oxidation yields **3**, whereas reduction yields **5**. Reaction a shows that reactive aldehydes can conjugate proteins by Schiff base formation. Reaction b shows that  $\alpha$ - $\beta$  unsaturated aldehydes, such as **4**, can additionally link proteins by conjugate addition.

an aldehyde generated from the peroxidation of  $\omega$ -6 polyunsaturated fatty acids (PUFAs), is cytotoxic, genotoxic, mutagenic, and hepatotoxic.

These aldehydes are significantly elevated in cells, plasma, and organ tissue when an organism is under oxidative stress.<sup>42</sup> Oxidative stress, while complex, can be viewed as an imbalance in the generation and destruction of reactive oxygen species generated by normal or pathological metabolic processes, including infections. The relationship between AD, PD, and 4-hydroxynonenal

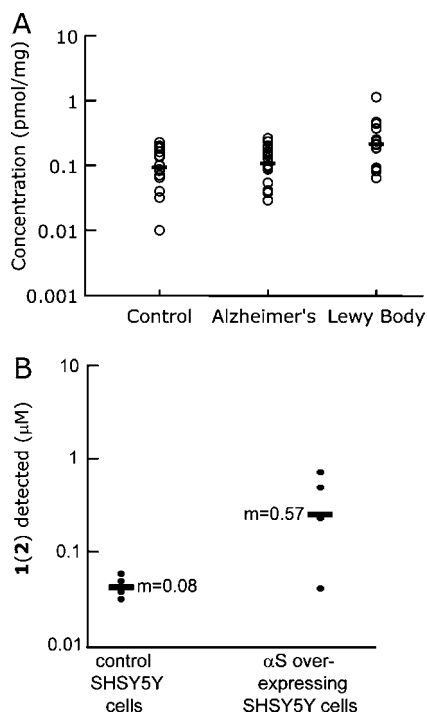


**FIGURE 2.** Quantification of cholesterol oxidation products *in vivo*. (A) Extraction of **1(2)** from 19 AD, 15 LBD, and 18 age matched control cortex tissue samples reveals elevated **1(2)** concentration in LBD brains (0.21 vs 0.09 pmol/mg). Concentrations of **1(2)** in AD brains (mean 0.12 pmol/mg) were not significantly elevated. (B) Concentration of **1(2)** in  $\alpha$ -synuclein overexpressing SHSY5Y cell culture was elevated (0.57  $\mu$ M) relative to control cells (0.075  $\mu$ M).

(Figure 1E, 4) illustrates this point.<sup>43</sup> The physiological concentration of **4** ranges from 0.1 to 1.0  $\mu$ M.<sup>44</sup> Its levels are elevated significantly in the brains of individuals with AD relative to age-matched controls.<sup>45</sup> Moreover, it has been detected immunohistochemically in AD amyloid plaques<sup>46</sup> and Parkinsonian Lewy bodies.<sup>47</sup>

### Inflammation-Linked Aldehydes Associated with Atherosclerosis Covalently Modify Proteins

We have provided evidence that the aldehyde-containing cholesterol 5,6-secosterols **1** and **2** (Figure 1E), which were recently discovered in the plaque material and plasma of patients with atherosclerosis, also may be important in AD and PD.<sup>48</sup> Because **1** and **2** interconvert by reversible Schiff base-mediated aldolization, the equilibrium mixture will be referred to as **1(2)**. *Ex vivo* activation of residual macrophages within human atheroma leads to a significant increase in secosterol levels. Their formation has been linked to the antibody-catalyzed water oxidation pathway that is itself activated by singlet dioxygen (<sup>1</sup>O<sub>2</sub>), which is generated by activated leukocytes.<sup>49–52</sup>

Secosterols **1(2)** and 4-hydroxynonenal (**4**) contain a large hydrophobic structure attached to an aldehyde that can covalently modify polypeptides and substantially alter their physical properties (**1(2)** are especially hydrophobic). Cholesterol, the precursor of **1(2)**, forms micelles at nanomolar concentrations.<sup>53</sup> Similarly, **1(2)** linked to a peptide could enhance peptide aggregation by mediating

micelle-like self-assembly. The aldehydes of **1**, **2**, and **4** can react with the  $\epsilon$ -amine of lysine, the N-terminal amine, or both to reversibly form Schiff bases (Figure 1E, reaction a). In contrast to **1(2)**, **4** has two reactive sites and can therefore cross-link proteins intra- or intermolecularly.<sup>54</sup> This results when a histidine or cysteine nucleophilic side chain from a protein adds to **4** by a 1,4 (Michael) addition<sup>54</sup> (Figure 1E, reaction b), followed by Schiff base formation utilizing the resulting aldehyde. Whereas the polypeptide–**1(2)** metabolite conjugates are envisioned to lower the critical concentration, **4** could initiate aggregation by intermolecular cross-linking.

### Cholesterol Aldehyde-Mediated Misfolding Can Be Traceless in Alzheimer's Disease

We have shown that **1(2)** is present in postmortem human brain samples (Figure 2A);<sup>55</sup> however the levels of **1(2)** in Alzheimer's brains and age-matched controls is not significantly different. Nonetheless, a transient increase in the levels of **1(2)** resulting from inflammation (trauma, infection) could initiate A $\beta$  amyloidogenesis, having effects on pathology long after the levels of **1(2)** have dropped to normal, because the fibrils so formed could trigger sporadic AD by acting as seeds for subsequent fibril formation. Such a scenario would explain the cholesterol- and inflammation-related risk factors associated with AD.

### Cholesterol Oxidation Products Are Elevated in Lewy Body Dementia Brains

In contrast to AD patients, Figure 2A demonstrates that DLB patients have significantly higher levels of **1(2)** (0.21 pmol/mg) than aged-matched controls (0.09 pmol/mg).<sup>56</sup> Thus, **1(2)** are significantly elevated in  $\alpha$ -synucleinopathies, suggesting that these metabolites influence aggregation.

Synucleinopathies have been linked to elevated  $\alpha$ -synuclein expression,<sup>57</sup> which in turn has been linked to the formation of reactive oxygen species (ROS),<sup>58</sup> which could lead to a vicious cycle in which oxidative metabolites accelerate  $\alpha$ -synuclein aggregation, inducing the generation of more reactive oxygen species.  $\alpha$ -Synuclein overexpression in SHSY5Y human dopaminergic neuroblastoma cells leads to an order of magnitude increase in **1(2)** concentration relative to control cells (Figure 2B, 0.57 vs 0.08  $\mu$ M).<sup>56</sup> Although high cholesterol is not an established risk factor for synucleinopathies,  $\alpha$ -synuclein is associated with cholesterol-rich regions of cell membranes.<sup>59</sup> This association, along with the elevated levels of **1(2)**, suggests that these metabolites could play an active role in the Lewy body pathogenesis.

### Oxidized Cholesterol Accelerates A $\beta$ Aggregation by Covalent Modification

If oxidized small molecules play a mechanistic role in promoting protein aggregation in humans, triggering misfolding diseases, they should accelerate A $\beta$  and  $\alpha$ -synuclein aggregation *in vitro*. We have found this to be the

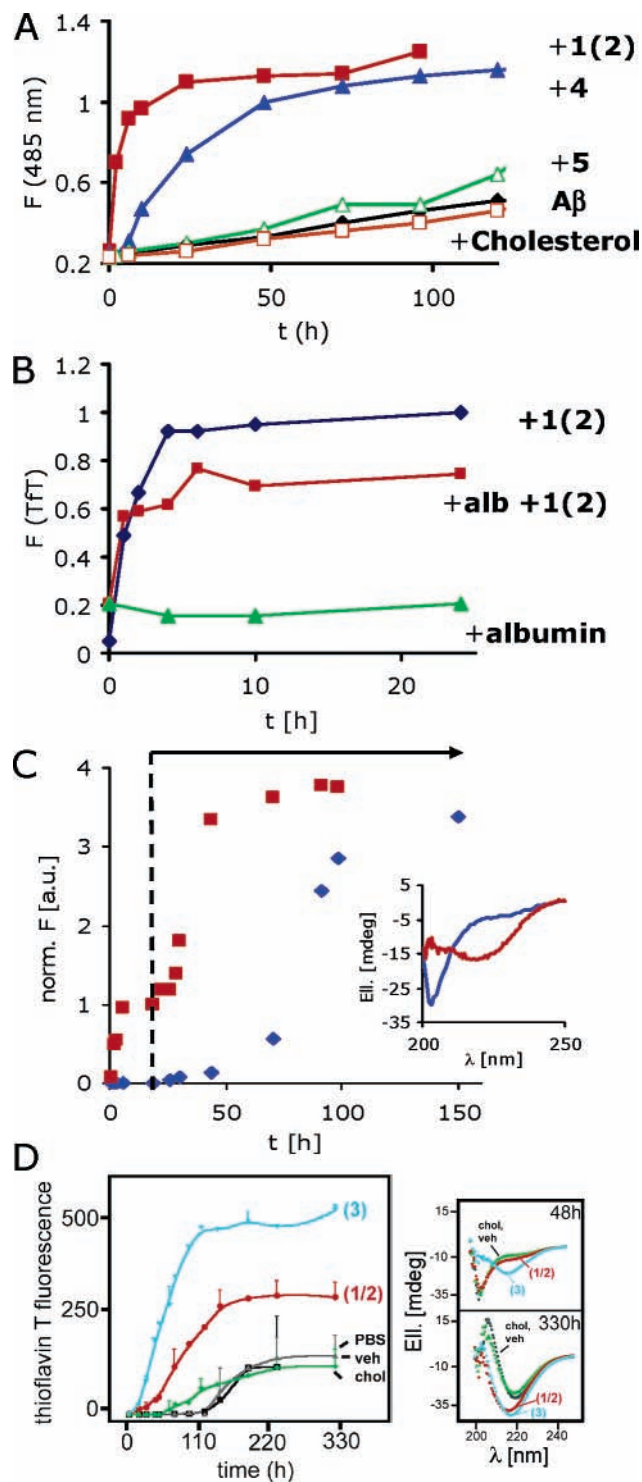


**FIGURE 3.** Lipid aldehydes accelerate aggregation. (A)  $A\beta$  1–40 (100  $\mu$ M) aggregation in the absence and presence of cholesterol, **1(2)**, **4**, and **5** (50  $\mu$ M), monitored by Tft fluorescence at 37  $^{\circ}$ C (300 mM NaCl, 50 mM sodium phosphate, pH 7.4) in a stagnant assay. (B) Albumin (15  $\mu$ M, 885  $\mu$ M in lysine residues) does not significantly inhibit the effect of **1(2)** (50  $\mu$ M) under the conditions described in panel A. (C)  $A\beta$  1–40 aggregation as described in panel A except that agitation (5 s every 30 min) was initiated after 19 h. The inset shows the CD spectra of  $A\beta$  1–40 after 1 (blue) and 150 h (red). (D) Increase in Tft fluorescence detecting  $\alpha$ -synuclein (25  $\mu$ M) aggregation is accelerated in the presence of **1(2)** (25  $\mu$ M, red) and **3** (blue) relative to cholesterol (green) and buffer (gray) controls. The inset shows the CD spectra of  $\alpha$ -synuclein after 48 and 330 h.

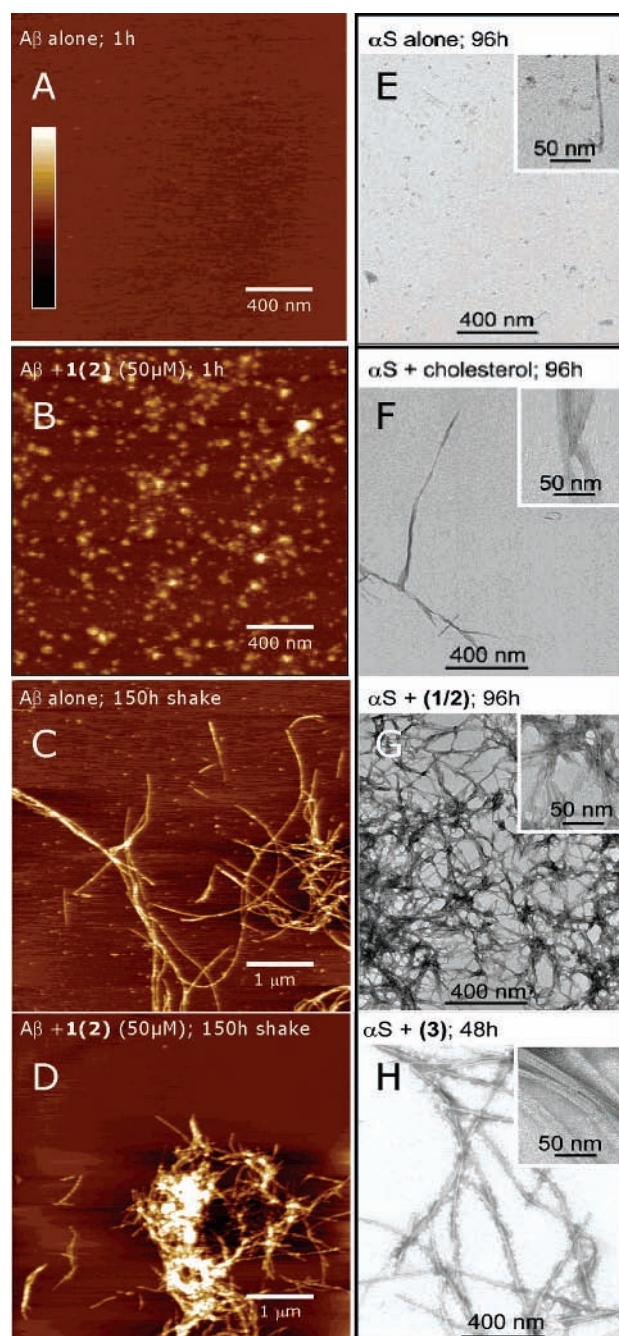


**FIGURE 4.** Aggregates formed by  $A\beta$  1–40 with agitation as described in Figure 3C. Spherical aggregates form rapidly in the presence (B) but not in the absence of **1(2)** (A). Final aggregates show fibrillar morphology (C, D). (E–H)  $\alpha$ -Synuclein forms mature fibrils under conditions described in Figure 3D within 48 h in the presence of **3** (H) and within 96 h in the presence of **1(2)** (G), whereas few, short fibrils are detected in cholesterol (F) and buffer controls (E) after 96 h. Height scale bars were (A, B) 0–20 nm and (C, D) 0–10 nm.

case.<sup>55,56,60</sup> Incubation of seed-free  $A\beta$  1–40 at neutral pH (pH 7.4, 300 mM NaCl, 37  $^{\circ}$ C) with **1(2)** leads to formation within less than 10 h of  $A\beta$  aggregates that bind the amyloidophilic dye thioflavin T (Tft). Under the same conditions, no Tft signal was observed in the absence of **1(2)** (Figure 3A). Likewise, 4-hydroxynonenal (**4**) induced aggregate formation, whereas cholesterol and ketoalcohol

(5) did not (Figure 3A). The presence of other prominent cerebrospinal fluid proteins, such as albumin, did not substantially inhibit the hastening of  $A\beta$  aggregation, demonstrating that, although **1(2)** likely forms Schiff bases with these competitor proteins, the process is reversible so the metabolites are still available to modify  $A\beta$  and accelerate its aggregation (Figure 3B). The physical properties of natively unfolded proteins are dramatically changed by covalent modification, unlike the situation for large globular proteins.

Atomic force microscopy demonstrates that aggregates of  $A\beta$  1–40 (100  $\mu\text{M}$ ) were not detected in the absence of **1(2)** (Figure 4A); however spherical  $A\beta$  1–40 aggregates with a diameter of 5–8 nm were formed within 1 h (Figure 4B) in the presence of **1(2)**, which are kinetically stable under quiescent conditions. To observe fibrillization (Figure 4C,D) of the spherical aggregates on a reasonable time scale, the reaction had to be agitated (Figure 3C). Fibrillar aggregates showed a predominantly  $\beta$ -sheet structure based on far-UV circular dichroism spectra (Figure 3C, inset). The spherical  $A\beta$  aggregates formed in the presence of **1(2)** under quiescent conditions also converted to fibrils upon addition of fibrillar seeds, indicating that the spherical aggregates are kinetically competent to form fibrils.<sup>55</sup>

### Oxidized Cholesterol Accelerates $\alpha$ -Synuclein Amyloidogenesis Apparently Noncovalently

Secosterols **1(2)** accelerate  $\alpha$ -synuclein aggregation in both stagnant and agitated assays.<sup>56</sup> The TFF signal increases over 72 h in samples of  $\alpha$ -synuclein (25  $\mu\text{M}$ ) in the presence of **1(2)** (25  $\mu\text{M}$ ), Figure 3D. In the presence of cholesterol or the vehicle buffer, no increase in TFF fluorescence was observed over 120 h, and the final TFF amplitude was much reduced, consistent with the EM data (Figures 4F,G). Our inability to detect  $\alpha$ -synuclein–**1(2)** adducts forced us to consider a noncovalent mechanism. To test such a mechanism, compound **3** was prepared by oxidizing the aldehyde functional group in **1(2)** to an acid that is incapable of Schiff base formation. Acid **3** hastened  $\alpha$ -synuclein aggregation even more than **1(2)** ( $t_{50} = 48$  h, Figure 3D), affording fibrils (cf. Figure 4E,H) with a predominantly  $\beta$ -sheet structure. Although we know that  $\alpha$ -synuclein forms a Schiff base with **1**, because  $\alpha$ -synuclein catalyzes the conversion of **1** into **2**,<sup>56</sup> this conjugate was not observed by mass spectrometry and was not essential for acceleration of  $\alpha$ -synuclein aggregation. The micellar properties of **1**, **2**, and **3** may be responsible for hastening  $\alpha$ -synuclein fibrillization. We are currently investigating this possibility.

### Hydrophobic Aldehyde Modification of the $A\beta$ Peptide Lowers Its Critical Concentration ( $K_c$ )

Increasing the hydrophobicity of a fibrillogenic peptide by metabolite modification could facilitate fibril formation by burial of large hydrophobic groups in the assemblies.<sup>61,62</sup> This would translate into a decrease in  $K_c$ , which would allow metabolite-modified peptides or a specific

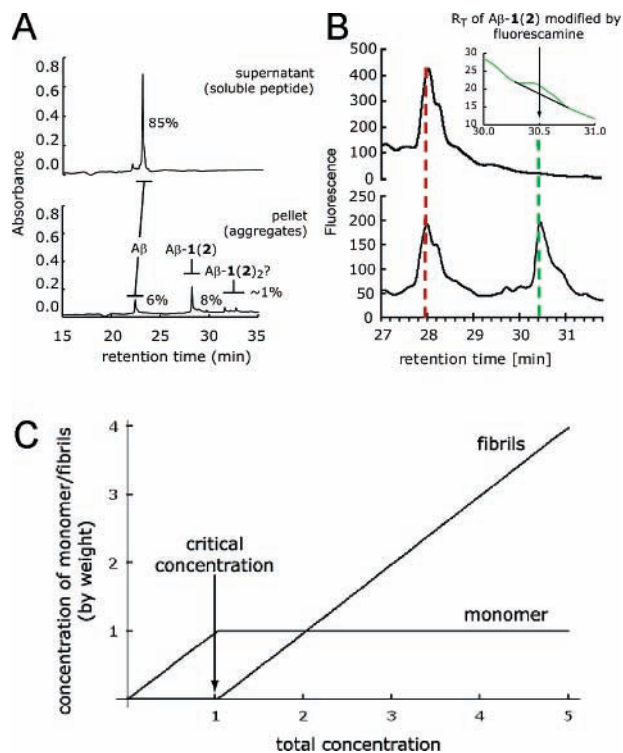


**FIGURE 5.** Oxidation products lower  $A\beta$  critical concentration ( $K_c$ ). (A) HPLC traces from the  $\text{NaBH}_4$ -reduced supernatant and pellet of  $A\beta$  (100  $\mu\text{M}$ ) incubated with **1(2)** (100  $\mu\text{M}$ ) for 3 h as in Figure 3A. (B) Same incubation (16 h) after which  $A\beta$  is derivatized with fluorescamine. Concentration of  $A\beta$ –**1(2)** in the supernatant was at most  $70 \pm 20$  nM. (C) Schematic representation of the concentrations of monomers and aggregates as a function of total peptide concentration. The maximal concentration of soluble peptide is equal to  $K_c$ .

stoichiometry of modified and unmodified peptides to form fibrils at lower concentrations than their unmodified counterparts. This could explain how  $A\beta$  forms fibrils at physiological concentrations ( $\sim 1$ – $10$  nM),<sup>63</sup> which are much lower than  $K_c$ 's reported for  $A\beta$  aggregation *in vitro* ( $\sim 1$ – $10$   $\mu\text{M}$ ).<sup>64,65</sup>

Since  $K_c$  is equal to the total concentration of soluble peptide after aggregation is complete, separating aggregated  $A\beta$  from soluble  $A\beta$  by ultracentrifugation is a convenient way of assessing the upper limit of  $K_c$ . Figure 5A shows HPLC chromatograms of supernatant and pellet fractions of an  $A\beta$  1–40 aggregation reaction in the presence of **1(2)** (50  $\mu\text{M}$ ).<sup>55</sup> The pellet has equal amounts of modified and unmodified  $A\beta$  after  $\text{NaBH}_4$  reduction of the Schiff base (Figure 5A,B, lower panels). No  $A\beta$ –**1(2)** conjugate was detected in the soluble fraction suggesting that the conjugate's  $K_c$  is very low. Both fractions also were derivatized with fluorescamine, which allowed detection of  $A\beta$  by HPLC down to a concentration of  $\sim 50$  nM. The small fraction of soluble  $A\beta$ –**1(2)** detected put an upper limit on  $K_c$  of  $70 \pm 20$  nM (Figure 5B).<sup>55</sup> Thus, modification by **1(2)** lowered the  $K_c$  of  $A\beta$  1–40 by approximately 100-fold. Modified  $A\beta$  1–40 also recruits unmodified  $A\beta$  1–40 to aggregate with it, since the pellet has equal amounts modified and unmodified  $A\beta$  peptide after  $\text{NaBH}_4$  reduction of the Schiff base (Figure 5A,B, lower panels). This

could occur either if aggregates consisting only of modified  $A\beta$  acted as a seed on which unmodified  $A\beta$  later adds or if modified and unmodified  $A\beta$  formed a “solid-solution”-type mixed oligomer in which modified and unmodified  $A\beta$  were both included within the fibril structure. The latter explanation would suggest that stabilizing interactions occur between the metabolite substructure on modified  $A\beta$  1–40 and unmodified  $A\beta$  1–40 in the aggregates preventing the dissociation of unmodified  $A\beta$ . In either case, the aggregates induced by  $A\beta$  modification can serve as templates for further fibril growth by addition of unmodified  $A\beta$ , as mentioned above.

## Lipid Oxidation Products Obviate $A\beta$ Nucleation by Forming Spherical Aggregates

Increases in amyloidogenic peptide hydrophobicity mediated by Schiff base formation with **1(2)** should cause the equilibrium constant  $K_n$  (Figure 1A) to decrease. Since  $K_n$  dictates the stability of the nucleus relative to monomers, this could profoundly change the mechanism of fibril formation. If  $K_n$  became lower than the peptide concentration, the nucleus would no longer be the highest energy species on the fibril formation pathway; the monomer would be. This would lead to an aggregation mechanism referred to as a downhill polymerization (Figure 6E, dotted line).

To test this hypothesis, we plotted the point of half-maximal Tft fluorescence ( $t_{50}$ ) on a logarithmic scale versus the starting peptide concentration. Since aggregation time scales with  $(n + 1)/2$  for a nucleated polymerization, the resulting slope would be  $-(n + 1)/2$ ,<sup>21</sup> whereas downhill polymerizations would yield a slope of  $-1$ .<sup>66</sup> We and others have used this approach to test the mechanisms of aggregation of several proteins.<sup>7,22</sup> Figure 6A shows the Tft fluorescence from the shaken  $A\beta$  1–40 aggregation reaction (5–100  $\mu\text{M}$ ) in the presence of **1(2)** (50  $\mu\text{M}$ ).<sup>60</sup> A plot of  $\log t_{50}$  vs  $\log [A\beta]$  for the first stage of aggregation (Figure 6B) exhibits a slope of  $-0.96$  ( $R^2 > 0.99$ ) indicating that the first stage of  $A\beta$  1–40 aggregation reaction, in which spherical aggregates are formed and which is the only stage observed in stagnant assays in the presence of metabolite,<sup>55</sup> is a downhill polymerization.<sup>60</sup>

The influence of metabolites **1(2)** on fibril elongation was also probed (Figure 6E, dashed line) by measuring fibril elongation rates, calculated from the initial slopes of aggregate growth in seeded aggregation assays.<sup>67</sup> Figure 6C shows the increase in Tft fluorescence of  $A\beta$  1–40 (20  $\mu\text{M}$ ) in the presence of 5%, 10%, and 20% (w/w) aggregation seeds, prepared by sonication of preformed  $A\beta$  1–40 fibrils. The initial slopes (Figure 6C,D) showed no dependence of the fibril growth rate on **1(2)**.<sup>60</sup>

## Aldehyde Scavengers Inhibit Schiff Base Hastened $A\beta$ but Not $\alpha$ -Synuclein Amyloidogenesis

Aldehyde-enabled Schiff base formation is critical for **1(2)** and **4** to accelerate  $A\beta$  aggregation.<sup>55</sup> Hence, it should be

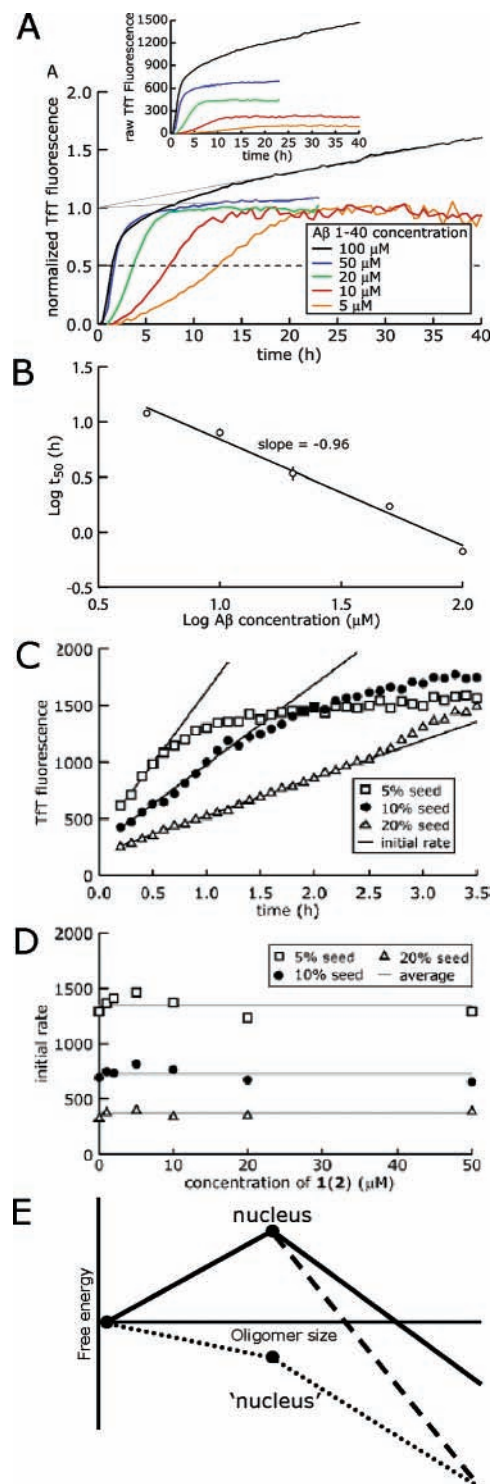


**FIGURE 6.** Lipid oxidation products induce aggregation by downhill polymerization. (A)  $A\beta$  1–40 concentration (5–100  $\mu\text{M}$ ) dependence of the first stage of its aggregation in the presence of **1(2)** (50  $\mu\text{M}$ ) under the conditions described in Figure 3A, except that it is agitated by shaking for 5 s every 10 min. (B) Time to 50% completion ( $t_{50}$ ) is plotted against  $A\beta$  concentration on a double logarithmic scale (slope =  $-0.96$ ,  $R^2 = 0.99$ ,  $n = 1$ ). (C) Aggregation of  $A\beta$  1–40 (50  $\mu\text{M}$ ) as described in Figure 5 seeded by the addition of 5%, 10%, and 20% sonicated fibrillar  $A\beta$  1–40. (D) Initial slopes for different concentrations of **1(2)** show no concentration dependence. (E) Free energy diagram for aggregation by a downhill polymerization mechanism (dotted line), compared to nucleated polymerization (solid line) and facilitated fibril growth (dashed line).

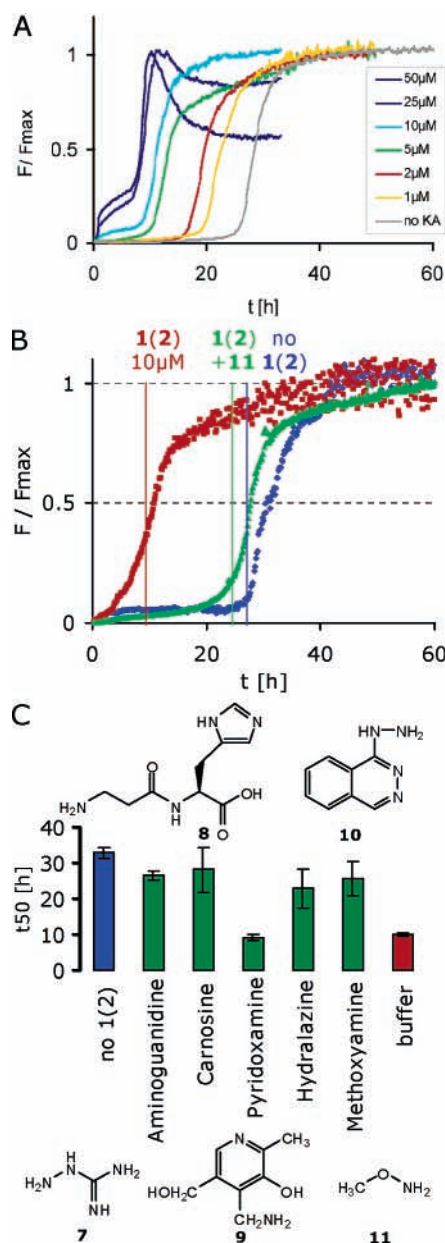


**FIGURE 7.** Acceleration of fibril formation by oxidative metabolites can be inhibited by aldehyde scavenging compounds. (A) The second stage of  $A\beta$  1–40 (50  $\mu$ M) aggregation, that is, fibril formation, is accelerated depending on concentration of **1(2)** (assay as in Figure 6A). (B)  $t_{50}$  in the presence of **1(2)** (10  $\mu$ M, red) can be prolonged by methoxyamine (100  $\mu$ M, green) back to the value observed in the absence of **1(2)** (blue). (C)  $t_{50}$  values for different compounds.

possible to eliminate their influence by using aldehyde-sequestering small molecules.<sup>68</sup> Several such molecules were added to an  $A\beta$  aggregation reaction at a 10-fold molar excess over **1(2)** (Figure 7B) to test the hypothesis that aldehyde-sequestering compounds can reverse metabolite-accelerated misfolding.<sup>60</sup> Aminoguanidine, carnosine, hydralazine, and methoxyamine (but not pyridoxamine) at 100  $\mu$ M were able to eliminate metabolite **1(2)** (10  $\mu$ M) acceleration of  $A\beta$  1–40 (50  $\mu$ M) aggregation, restoring the aggregation rate to that observed in the absence of **1(2)** (Figure 7A–C). Therefore, aldehyde carbonyl-trapping therapeutic strategies, which are already

under examination for other diseases,<sup>68,69</sup> could be effective in combating sporadic Alzheimer's disease. Analogous studies with  $\alpha$ -synuclein revealed that the aldehyde sequestering compounds did not eliminate oxidative metabolite accelerated misfolding,<sup>56</sup> supporting the hypothesis that **1(2)**-mediated acceleration of  $\alpha$ -synuclein aggregation occurs predominantly by a noncovalent mechanism.

## Conclusion

Oxidized hydrophobic membrane components hasten  $A\beta$  and  $\alpha$ -synuclein aggregation, associated with AD and synucleinopathies, by covalent and noncovalent mechanisms, respectively. Thus, these may be a new class of risk factors and potential prevention and intervention targets in neurodegenerative diseases. The aldehydes discussed herein probably only represent a small fraction of the oxidized small molecule pool that can trigger protein misfolding in sporadic amyloid diseases, which are the clinically most important diseases of the brain.

## References

- (1) Cohen, E.; Bieschke, J.; Perciavalle, R. M.; Kelly, J. W.; Dillin, A. Opposing activities protect against age onset proteotoxicity. *Science*, in press.
- (2) Sipe, J. D.; Cohen, A. S. Review: history of the amyloid fibril. *J. Struct. Biol.* **2000**, *130*, 88–98.
- (3) Selkoe, D. J. Folding proteins in fatal ways. *Nature* **2003**, *426*, 900–904.
- (4) Goedert, M. Alpha-synuclein and neurodegenerative diseases. *Nat. Rev.* **2001**, *2*, 492–501.
- (5) Sekijima, Y.; Wiseman, R. L.; Matteson, J.; Hammarstrom, P.; Miller, S. R.; Sawkar, A. R.; Balch, W. E.; Kelly, J. W. The biological and chemical basis for tissue-selective amyloid disease. *Cell* **2005**, *121*, 73–85.
- (6) Johnson, S. M.; Wiseman, R. L.; Sekijima, Y.; Green, N. S.; Adamski-Werner, S. L.; Kelly, J. W. Native state kinetic stabilization as a strategy to ameliorate protein misfolding diseases: a focus on the transthyretin amyloidoses. *Acc. Chem. Res.* **2005**, *38*, 911–921.
- (7) Hurshman, A. R.; White, J. T.; Powers, E. T.; Kelly, J. W. Transthyretin aggregation under partially denaturing conditions is a downhill polymerization. *Biochemistry* **2004**, *43*, 7365–7381.
- (8) Cohen, F. E.; Kelly, J. W. Therapeutic approaches to protein-misfolding diseases. *Nature* **2003**, *426*, 905–909.
- (9) Hammarstrom, P.; Wiseman, R. L.; Powers, E. T.; Kelly, J. W. Prevention of transthyretin amyloid disease by changing protein misfolding energetics. *Science* **2003**, *299*, 713–716.
- (10) Dobson, C. M. Protein misfolding, evolution, and disease. *Trends Biochem. Sci.* **1999**, *24*, 329–332.
- (11) Fowler, D. M.; Koulouf, A. V.; Alory-Jost, C.; Marks, M. S.; Balch, W. E.; Kelly, J. W. Functional amyloid formation within mammalian tissue. *PLoS Biol.* **2006**, *4*, e6.
- (12) Petkova, A. T.; Ishii, Y.; Balbach, J. J.; Antzutkin, O. N.; Leapman, R. D.; Delaglio, F.; Tycko, R. A structural model for Alzheimer's beta-amyloid fibrils based on experimental constraints from solid state NMR. *Proc. Natl. Acad. Sci. U.S.A.* **2002**, *99*, 16742–16747.
- (13) Nelson, R.; Sawaya, M. R.; Balbirnie, M.; Madsen, A. O.; Riekel, C.; Grothe, R.; Eisenberg, D. Structure of the cross-beta spine of amyloid-like fibrils. *Nature* **2005**, *435*, 773–778.
- (14) Luhrs, T.; Ritter, C.; Adrian, M.; Riek-Loher, D.; Bohrmann, B.; Döbeli, H.; Schubert, D.; Riek, R. 3D structure of Alzheimer's amyloid-beta(1–42) fibrils. *Proc. Natl. Acad. Sci. U.S.A.* **2005**, *102*, 17342–17347.
- (15) Walsh, D. M.; Hartley, D. M.; Kusumoto, Y.; Fezoui, Y.; Condron, M. M.; Lomakin, A.; Benedek, G. B.; Selkoe, D. J.; Teplow, D. B. Amyloid beta-protein fibrillogenesis. Structure and biological activity of protofibrillar intermediates. *J. Biol. Chem.* **1999**, *274*, 25945–25952.
- (16) Lashuel, H. A.; Hartley, D.; Petre, B. M.; Walz, T.; Lansbury, P. T. Neurodegenerative disease: Amyloid pores from pathogenic mutations. *Nature* **2002**, *418*, 291.

- (17) Kaye, R.; Head, E.; Thompson, J. L.; McIntire, T. M.; Milton, S. C.; Cotman, C. W.; Glabe, C. G. Common structure of soluble amyloid oligomers implies common mechanism of pathogenesis. *Science* **2003**, *300*, 486–489.
- (18) Lambert, M. P.; Barlow, A. K.; Chromy, B. A.; Edwards, C.; Freed, R.; Liosatos, M.; Morgan, T. E.; Rozovsky, I.; Trommer, B.; Viola, K. L.; Wals, P.; Zhang, C.; Finch, C. E.; Krafft, G. A.; Klein, W. L. Diffusible, nonfibrillar ligands derived from A $\beta$ 1-42 are potent central nervous system neurotoxins. *Proc. Natl. Acad. Sci. U.S.A.* **1998**, *95*, 6448–6453.
- (19) Harper, J. D.; Lansbury, P. T., Jr. Models of amyloid seeding in Alzheimer's disease and scrapie: mechanistic truths and physiological consequences of the time-dependent solubility of amyloid proteins. *Ann. Rev. Biochem.* **1997**, *66*, 385–407.
- (20) Oosawa, F.; Asakura, S. *Thermodynamics of the Polymerization of Protein*; Academic Press: London, 1975.
- (21) Ferrone, F. Analysis of protein aggregation kinetics. *Methods Enzymol.* **1999**, *309*, 256–274.
- (22) Chen, S.; Ferrone, F. A.; Wetzel, R. Huntington's disease age-onset linked to polyglutamine aggregation nucleation. *Proc. Natl. Acad. Sci. U.S.A.* **2002**, *99*, 11884–11889.
- (23) Teplow, D. B. Structural and kinetic features of amyloid beta-protein fibrillogenesis. *Amyloid* **1998**, *5*, 121–142.
- (24) Bossy-Wetzel, E.; Schwarzenbacher, R.; Lipton, S. A. Molecular pathways to neurodegeneration. *Nat. Med.* **2004**, *10 Suppl*, S2–9.
- (25) Nilsson, M. R.; Driscoll, M.; Raleigh, D. P. Low levels of asparagine deamidation can have a dramatic effect on aggregation of amyloidogenic peptides: implications for the study of amyloid formation. *Protein Sci.* **2002**, *11*, 342–349.
- (26) Uchida, K.; Stadtman, E. R. Modification of histidine residues in proteins by reaction with 4-hydroxynonenal. *Proc. Natl. Acad. Sci. U.S.A.* **1992**, *89*, 4544–4548.
- (27) Eikelenboom, P.; Bate, C.; van Gool, W. A.; Hoozemans, J. J. M.; Rozemuller, J. M.; Veerhuis, R.; Williams, A. Neuroinflammation in Alzheimer's Disease and Prion Disease. *Glia* **2002**, *40*, 232–239.
- (28) Lye, T. C.; Shores, E. A. Traumatic brain injury as a risk factor for Alzheimer's disease: a review. *Neuropsychol. Rev.* **2000**, *10*, 115–129.
- (29) Culpan, D.; MacGowan, S. H.; Ford, J. M.; Nicoll, J. A.; Griffin, W. S.; Dewar, D.; Cairns, N. J.; Hughes, A.; Kehoe, P. G.; Wilcock, G. K. Tumour necrosis factor-alpha gene polymorphisms and Alzheimer's disease. *Neurosci. Lett.* **2003**, *350*, 61–65.
- (30) Papassotiropoulos, A.; Bagli, M.; Jessen, F.; Bayer, T. A.; Maier, W.; Rao, M. L.; Heun, R. A genetic variation of the inflammatory cytokine interleukin-6 delays the initial onset and reduces the risk for sporadic Alzheimer's disease. *Ann. Neurol.* **1999**, *45*, 666–668.
- (31) Montine, T. J.; Neely, M. D.; Quinn, J. F.; Beal, M. F.; Markesbery, W. R.; Roberts, L. J.; Morrow, J. D. Lipid peroxidation in aging brain and Alzheimer's disease. *Free Radical Biol. Med.* **2002**, *33*, 620–626.
- (32) Arlt, S.; Beisiegel, U.; Kontush, A. Lipid peroxidation in neurodegeneration: new insights into Alzheimer's disease. *Curr. Opin. Lipidol.* **2002**, *13*, 289–294.
- (33) in 't Veld, B. A.; Ruitenber, A.; Hofman, A.; Launer, L. J.; van Duijn, C. M.; Stijnen, T.; Breteler, M. M.; Stricker, B. H. Nonsteroidal antiinflammatory drugs and the risk of Alzheimer's disease. *N. Engl. J. Med.* **2001**, *345*, 1515–1521.
- (34) Hirsch, E. C.; Breidert, T.; Rousselet, E.; Hunot, S.; Hartmann, A.; Michel, P. P. The role of glial reaction and inflammation in Parkinson's disease. *Ann. N. Y. Acad. Sci.* **2003**, *991*, 214–228.
- (35) Jenner, P. Oxidative stress in Parkinson's disease. *Ann. Neurol.* **2003**, *52*, S26–S36.
- (36) Mackenzie, I. R. Cortical inflammation in dementia with Lewy bodies. *Arch. Neurol.* **2001**, *58*, 519–520.
- (37) Serra, J. A.; Dominguez, R. O.; de Lustig, E. S.; Guareschi, E. M.; Famulari, A. L.; Bartolome, E. L.; Marschoff, E. R. Parkinson's disease is associated with oxidative stress: comparison of peripheral antioxidant profiles in living Parkinson's, Alzheimer's and vascular dementia patients. *J. Neural Transm.* **2001**, *108*, 1135–1148.
- (38) Esterbauer, H. In *Free Radicals in Liver Injury*; Poli, G., Cheeseman, K. H., Dianzani, M. U., Slater, T. F., Eds.; IRL Press: Oxford, U.K. 1982; pp 29–47.
- (39) Esterbauer, H. In *Free Radicals, Lipid Peroxidation and Cancer*; McBrien, D. C. H., Slater, T. F., Eds.; Academic Press: London, 1982; p 101.
- (40) Frankel, E. N. Volatile lipid oxidation products. *Prog. Lipid Res.* **1982**, *22*, 1–33.
- (41) Grosch, W. In *Autoxidation of Unsaturated Lipids*; Chan, H. W. S., Ed.; Academic Press: London, 1987.
- (42) Esterbauer, H.; Zollner, H.; Schaur, R. J. In *Membrane Lipid Oxidation*; Vigo-Pelfrey, C., Ed.; CRC Press: Boston, MA, 1990; pp 239–268.
- (43) Zarkovic, K. 4-Hydroxynonenal and neurodegenerative diseases. *Mol. Aspects Med.* **2003**, *24*, 293–303.
- (44) Esterbauer, H.; Schaur, R. J.; Zollner, H. Chemistry and biochemistry of 4-hydroxynonenal, malonaldehyde and related aldehydes. *Free Radical Biol. Med.* **1991**, *11*, 81–128.
- (45) Sayre, L. M.; Zelasko, D. A.; Harris, P. L. R.; Perry, G.; Salomon, R. G.; Smith, M. A. 4-Hydroxynonenal-derived advanced lipid peroxidation end products are increased in Alzheimer's disease. *J. Neurochem.* **1997**, *68*, 2092–2097.
- (46) Ando, Y.; Brannstrom, T.; Uchida, K.; Nyhlin, N.; Nasman, B.; Suhr, O.; Yamashita, T.; Olsson, T.; El Salhy, M.; Uchino, M.; Ando, M. Histological detection of 4-hydroxynonenal protein in Alzheimer amyloid. *J. Neurol. Sci.* **1998**, *156*, 172–176.
- (47) Yoritaka, A.; Hattori, N.; Uchida, K.; Tanaka, M.; Stadtman, E. R.; Mizuno, Y. Immunohistochemical detection of 4-hydroxynonenal protein adducts in Parkinson disease. *Proc. Natl. Acad. Sci. U.S.A.* **1996**, *93*, 2696–2701.
- (48) Wentworth, P., Jr.; Nieva, J.; Galve, R.; Takeuchi, C.; Wenworth, A. D.; Dilley, R. B.; DeLaria, G. A.; Saven, A.; Babior, B. M.; Janda, K. D.; Eschenmoser, A.; Lerner, R. A. Evidence for ozone formation in human atherosclerotic arteries. *Science* **2003**, *302*, 1053–1056.
- (49) Wentworth, P., Jr.; Jones, L. H.; Wentworth, A. D.; Zhu, X.; Larsen, N. A.; Wilson, I. A.; Xu, X.; Goddard, W. A., 3rd; Janda, K. D.; Eschenmoser, A.; Lerner, R. A. Antibody catalysis of the oxidation of water. *Science* **2001**, *293*, 1806–1811.
- (50) Wentworth, P., Jr.; McDunn, J. E.; Wentworth, A. D.; Takeuchi, C.; Nieva, J.; Jones, T.; Bautista, C.; Ruedi, J. M.; Gutierrez, A.; Janda, K. D.; Babior, B. M.; Eschenmoser, A.; Lerner, R. A. Evidence for antibody-catalyzed ozone formation in bacterial killing and inflammation. *Science* **2002**, *298*, 2195–2199.
- (51) Datta, D.; Vaidehi, N.; Xu, X.; Goddard, W. A., 3rd Mechanism for antibody catalysis of the oxidation of water by singlet dioxygen. *Proc. Natl. Acad. Sci. U.S.A.* **2002**, *99*, 2636–2641.
- (52) Babior, B. M.; Takeuchi, C.; Ruedi, J.; Gutierrez, A.; Wentworth, P., Jr. Investigating antibody-catalyzed ozone generation by human neutrophils. *Proc. Natl. Acad. Sci. U.S.A.* **2003**, *100*, 3031–3034.
- (53) Haberland, M. E.; Reynolds, J. A. Self-association of cholesterol in aqueous solution. *Proc. Natl. Acad. Sci. U.S.A.* **1973**, *70*, 2313–2316.
- (54) Sayre, L. M.; Smith, M. A.; Perry, G. Chemistry and biochemistry of oxidative stress in neurodegenerative disease. *Curr. Med. Chem.* **2001**, *8*, 721–738.
- (55) Zhang, Q.; Powers, E. T.; Nieva, J.; Huff, M. E.; Dendle, M. A.; Bieschke, J.; Glabe, C. G.; Eschenmoser, A.; Wentworth, P., Jr.; Lerner, R. A.; Kelly, J. W. Metabolite-initiated protein misfolding may trigger Alzheimer's disease. *Proc. Natl. Acad. Sci. U.S.A.* **2004**, *101*, 4752–4757.
- (56) Bosco, D. A.; Fowler, D. M.; Zhang, Q.; Nieva, J.; Powers, E. T.; Wentworth, P., Jr.; Lerner, R. A.; Kelly, J. W. Elevated levels of oxidized cholesterol metabolites in Lewy body disease brains accelerate alpha-synuclein fibrilization. *Nat. Chem. Biol.* **2006**, *2*, 249–253.
- (57) Singleton, A. B.; Farrer, M.; Johnson, J.; Singleton, A.; Hague, S.; Kachergus, J.; Hulihan, M.; Peuralinna, T.; Dutra, A.; Nussbaum, R.; Lincoln, S.; Crawley, A.; Hanson, M.; Maraganore, D.; Adler, C.; Cookson, M. R.; Muenter, M.; Baptista, M.; Miller, D.; Blancato, J.; Hardy, J.; Gwinn-Hardy, K. alpha-Synuclein locus triplication causes Parkinson's disease. *Science* **2003**, *302*, 841.
- (58) Junn, E.; Mouradian, M. M. Human alpha-synuclein over-expression increases intracellular reactive oxygen species levels and susceptibility to dopamine. *Neurosci. Lett.* **2002**, *320*, 146–150.
- (59) Fortin, D. L.; Troyer, M. D.; Nakamura, K.; Kubo, S.; Anthony, M. D.; Edwards, R. H. Lipid rafts mediate the synaptic localization of alpha-synuclein. *J. Neurosci.* **2004**, *24*, 6715–6723.
- (60) Bieschke, J.; Zhang, Q.; Powers, E. T.; Lerner, R. A.; Kelly, J. W. Oxidative metabolites accelerate Alzheimer's amyloidogenesis by a two-step mechanism, eliminating the requirement for nucleation. *Biochemistry* **2005**, *44*, 4977–4983.
- (61) Bitan, G.; Vollers, S. S.; Teplow, D. B. Elucidation of primary structure elements controlling early amyloid beta-protein oligomerization. *J. Biol. Chem.* **2003**, *278*, 34882–34889.
- (62) Chiti, F.; Stefani, M.; Taddei, N.; Ramponi, G.; Dobson, C. M. Rationalization of the effects of mutations on peptide and protein aggregation rates. *Nature* **2003**, *424*, 805–808.
- (63) Naslund, J.; Schierhorn, A.; Hellman, U.; Lannfelt, L.; Roses, A. D.; Tjernberg, L. O.; Silberring, J.; Gandy, S. E.; Winblad, B.; Greengard, P.; Nordstedt, C.; Terenius, L. Relative abundance of Alzheimer A beta amyloid peptide variants in Alzheimer disease and normal aging. *Proc. Natl. Acad. Sci. U.S.A.* **1994**, *91*, 8378–8382.



- (64) Jarrett, J. T.; Berger, E. P.; Lansbury, P. T., Jr. The carboxy terminus of the beta amyloid protein is critical for the seeding of amyloid formation: implications for the pathogenesis of Alzheimer's disease. *Biochemistry* **1993**, *32*, 4693–4697.
- (65) Sengupta, P.; Garai, K.; Sahoo, B.; Shi, Y.; Callaway, D. J. E.; Maiti, S. The Amyloid  $\beta$  Peptide ( $A\beta_{1-40}$ ) Is Thermodynamically Soluble at Physiological Concentrations. *Biochemistry* **2003**, *42*, 10506–10513.
- (66) Goldstein, R. F.; Stryer, L. Cooperative polymerization reactions. Analytical approximations, numerical examples, and experimental strategy. *Biophys. J.* **1986**, *50*, 583–599.
- (67) Collins, S. R.; Douglass, A.; Vale, R. D.; Weissman, J. S. Mechanism of prion propagation: amyloid growth occurs by monomer addition. *PLoS Biol.* **2004**, *2*, e321.
- (68) Burcham, P. C.; Kaminskas, L. M.; Fontaine, F. R.; Petersen, D. R.; Pyke, S. M. Aldehyde-sequestering drugs: tools for studying protein damage by lipid peroxidation products. *Toxicology* **2002**, *181–182*, 229–236.
- (69) Shapiro, H. K. Carbonyl-trapping therapeutic strategies. *Am. J. Ther.* **1998**, *5*, 323–353.

AR0500766